Materials Research Proceedings 44 (2024) 124-133 https://doi.org/10.21741/9781644903254-14

Design and simulation of cross wedge rolling process for hollow motor shaft

HAN M.[1,2,a], LIU J.X.[1,2], SHI M.J.[1,2], SONG H.W.[1], ZHANG S.H.[1] and CHENG M.[1,b *]

[1] Institute of Metal Research, Chinese Academy of Sciences, Shi-changxu Innovation Center for Advanced Materials, Shenyang 110016, China

[2] School of Materials Science and Engineering, University of Science and Technology of China, Shenyang 110016, China

[a]mhan22s@imr.ac.cn, [b]mcheng@imr.ac.cn

Keywords: Hollow Motor Shaft, Cross Wedge Rolling, Hollow Billet, Numerical Simulation

Abstract. Nowadays, electric cars are experiencing rapid development, in which the production of motor shaft is one of the important parts. The cross wedge rolling (CWR) process is expected to be an efficient and material-saving production method for motor shaft production. Traditional motor shafts are manufactured by forging and machining, which inevitably causes material waste. While using the CWR method to produce the motor shaft, the forming accuracy can be improved, keeping the material performance. It's possible to manufacture the hollow motor shaft billet directly and reducing the production cost greatly. Because of the asymmetric geometry profile of the motor shaft, the force is unbalanced during the forming process. The thermo-mechanical coupling finite element simulation is used to design and optimize the flat CWR tools. Then, the distribution of stress, strain, damage and temperature during the CWR process are analyzed. The traditional CWR process will easily cause central defects of the shaft such as micropores and voids. The hollow billet is used in the study. It helps to avoid such defects, also can be a new method to deal with the hollow motor shafts by CWR. Some disadvantages of traditional manufacture can be overcome.

Introduction

Motor shaft is a classic transmission shaft, and its demand is increasing with the development of electric cars. The hollow motor shaft has three advantages: low moment of inertia, lightweight structure and convenient defect detection, which is the mainstream trend of future development. The motor shaft has the characteristic of multiple steps, and the traditional manufacturing process is mechanical processing. The inner hole needs to be processed by deep hole processing, which leads to low material utilization and high processing difficulty. The cross wedge rolling (CWR) technology is a near-net shape metal working process with high forming precision and small cutting dimension allowance for forming the shaft parts [1,2]. Therefore, the use of CWR technology is expected to solve the above problems. However, there are two difficulties in producing hollow shafts for CWR. One is how to ensure the dimensional accuracy of the surface and inner hole of hollow shaft. The other one is how to rolling asymmetric structures [3,4].

The research on the hollow shaft manufactured by CWR is divided into two types: with mandrel and without mandrel [5-7]. Among them, using a mandrel can control the accuracy of the inner hole size, but the selection of mandrel size can only rely on experience, making tool design inconvenient. When the inner hole diameter is small, rolling without a mandrel can also obtain a rolled piece with roughly accurate inner hole size, and then simple processing of the inner hole can

meet the requirements. Hollow motor shafts mostly use smaller inner hole sizes, so rolling without mandrel has the advantage of improving production efficiency [8].

At the same time, the motor shaft is asymmetric, and the traditional CWR mostly adopts double pieces symmetrical rolling method. However, due to the long length of the motor shaft, limited by the size of the CWR rolling mill, single piece forming can only be used. It leads to the asymmetric step characteristics at both ends of the motor shaft, which are prone to axial force imbalance during the forming process, and the rolled piece is flattened after being skewed, resulting in rolling failure. Therefore, in the process of tool design, attention should be paid to the issue of axial force balance [9,10].

In this paper the changes in temperature, stress, and strain of hollow shaft parts during cross wedge rolling were analyzed through tool design and finite element simulation of motor shafts, providing guidance for actual production.

Tool design and simulation of CWR process

Tool Design for target motor shaft. Fig. 1 shows the target workpiece (rough motor shaft). It can be observed that the shaft has asymmetric features: the steps at both ends are asymmetric and fewer steps on the left and more steps (which have significant difference in diameters) on the right. At the same time, there is a narrow and high step in the middle of shaft. Therefore, axial force balance and forming method of narrow step had to be considered before the rolling tools are designed.

Fig. 2 shows the CWR tool with special design. For the forming of narrow step, using the traditional CWR tool design method will result in excessive processing volume, so special tool design is needed to squeeze the narrow steps into shape. The metal flow during the extrusion process should not be too large, which can be solved through tool design: the billet is slowly divided in the initial stage of wedging, and then formed with a smaller spreading angle. The position of dividing the billet needs to be calculated through the volume of narrow steps. In order to maintain axial force stability at the positions where asymmetric steps are formed at both ends, the tool was designed for the left step to be formed in two stages.

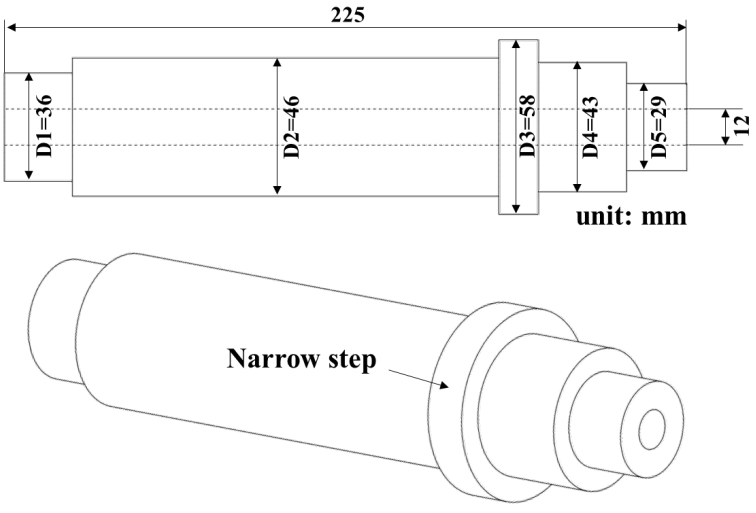

Fig. 1. Target rolled workpiece.

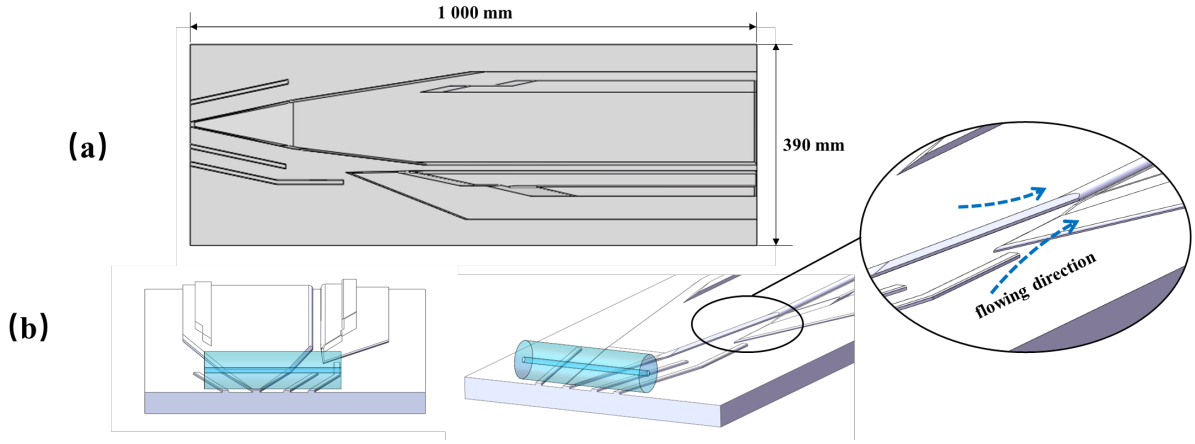

Fig. 2. Top view and special design of tools.

Finite element modeling. Finite element software DEFORM-3D was used for the simulation. The billet and tools were established, and their assembly relationship was adjusted, as shown in Fig. 3. Finally, the STL. format file was imported into the finite element software and simulation parameters were set further.

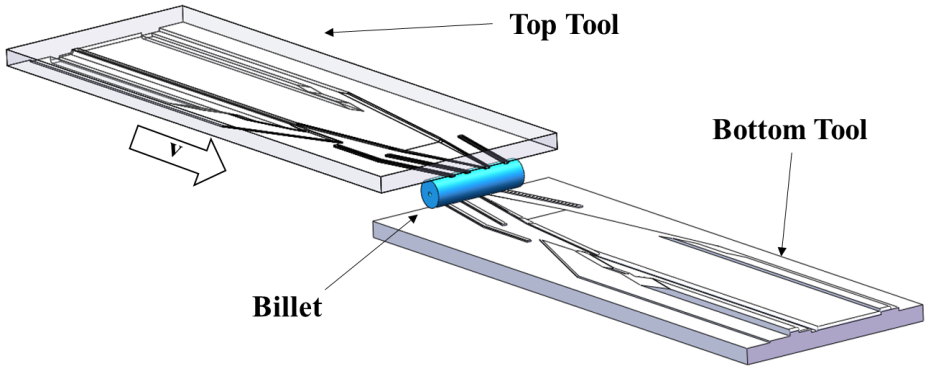

Fig. 3. Schematic diagram of assembly relationship between tools and billet.

During the CWR process of forming asymmetric parts, there are both radial compression and axial extension, as well as lateral extension. This results in non-linear stress-strain behavior of the material during the deformation process, as well as non-linear strain and displacement. The boundary conditions are very complex. Taking into account the above factors, establish a finite element model that conforms to the real forming process and make the following assumptions:

1. The plastic deformation of the billet is large, and its elastic deformation is ignored. It is set as a rigid plastic body, and the material model is selected from the 45 steel in the software material library.

2. Compared to the plastic deformation of the billet at high temperatures, the elastic deformation of the tool is too small to be ignored, and both sides of the tool can be regarded as rigid bodies.

3. In actual production, the friction groove can effectively avoid the phenomenon of slipping between the rolled piece and the tool. The friction type is selected as shear friction, and a higher friction coefficient (f=1.5) will be set.

4. The rolling process has a short duration, and the heat transfer coefficient between the billet and the environment, as well as the tool, can be considered as a constant value.

And the main parameters used in the simulation are shown in Table 1.

Table 1. Parameters used in the simulation.

Parameters	Number
Environment and tool temperature	20 ℃
Environmental thermal conductivity coefficient	0.02 N/(mm·s·℃)
Thermal conductivity coefficient of tools and billet	12 N/(mm·s·℃)
Rolling speed	300 mm/s
Billet temperature	1 000 ℃
Damage model	Normalized Cockroft & Latham: $f = \int_0^{\varepsilon} \frac{\sigma_1}{\sigma_i} d\varepsilon$

Results and discussion

Analysis of dimensional accuracy of rolled piece. During the rolling process, the surface of the billet comes into direct contact with the tool, generating a fast temperature drop. The surface metal is sensitive to temperature changes, and the plasticity and flowability of the material are affected by temperature, leading to rolling failure. Therefore, temperature of the billet and the rolling speed are the key factors affecting the dimensional accuracy of the rolled piece. The rolling speed should not be too low, and the selected rolling speed for this study is 300 mm/s. The simulation results of the rolled piece at 1000℃ are shown in Fig. 4.

Observing the morphology of the rolled piece, the size of the inner hole varies in a wavy shape, with a diameter of 3.4 mm at the narrowest point and 14.6 mm at the widest point. The initial diameter of the inner hole of billet was 7.5 mm (Calculate the approximate value based on the principle of volume invariance). The rolling force caused the billet to elongate towards both ends, and the diameter of the inner hole in the wedged position reached its maximum. The diameter of the inner hole decreases due to radial compression at both ends. There was no collapse in the inner hole, so the subsequent precision machining steps can be simplified. The dimensions of each step from left to right on the outer diameter of the rolled piece are set to D1-D5, as shown in Fig. 1. The comparison between the target size and the simulated size is shown in Table 2. The outer diameter deviation values are all less than 0.8 %, which proves that the external dimensions meet the requirements. Both ends of the material head have concave centers, but none of them affect the required part of the rolled piece. Therefore, the size of the rolled piece simulated by finite element method meets the target requirements, providing guidance for the experiment.

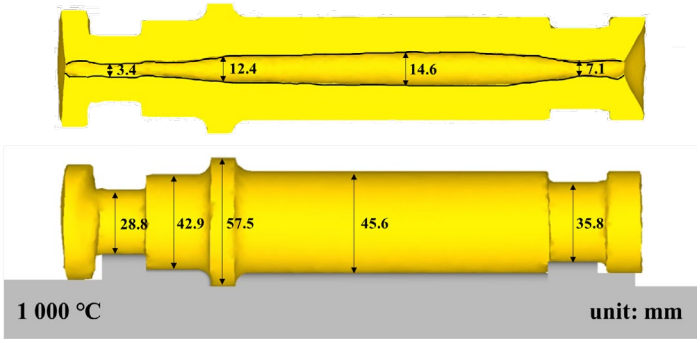

Fig. 4. The rolled workpiece at 1000℃.

Table 2. Target and simulation results of the selected cross-sections.

Position	Target (mm)	Simulation (mm)	Deviation (%)
D1	28.8	29	0.7
D2	42.9	43	0.2
D3	57.5	58	0.8
D4	45.6	46	0.8
D5	35.8	36	0.6

Analysis of temperature and stress. The CWR process lasts about 5.3 seconds, so it is of great significance to investigate the temperature changes of the billet. Fig. 5, 6 and 7 show the simulation results at a rolling temperature of 1000℃ and a rolling speed of 300 mm/s, when the rolling speed is high, the collapse of hollow shaft may occur [11]. Fig. 5(a) shows the temperature changes on the surface and cross-section during the wedging process of the rolled piece; Fig. 5(b) shows the stress changes on the surface and cross-section during the wedging process of the rolled piece. It can be clearly observed that there is a significant temperature difference between the surface and the center of the rolled piece. The surface of the billet directly contacts the tool, and the effect of heat transfer reduces the surface temperature. However, plastic deformation occurs inside due to compression, and the deformation energy is converted into heat energy, leading to an increase in temperature. The most significant decrease in temperature occurs when the rolled piece comes into contact with the wedge first, and it is also the part with the largest deformation.

Fig. 6(a) and 6(b) respectively show the temperature and stress changes on the surface and cross-section of the rolled piece during the intermediate stage of rolling. It can be seen that the surface temperature has significantly decreased and the core temperature has increased. The stress is mainly concentrated at the position where the surface contacts the tool.

Fig. 7(a) and 7(b) respectively show the temperature and stress changes on the surface and cross-section of the rolled piece during the end of rolling stage. The temperature from the surface to the core is distributed in a stepped pattern, but there is still a certain amount of high temperature on the right side of the narrow step. This is because the rolled piece is subjected to a left axial force, and the left side is in close contact with the tool, resulting in a rapid temperature decrease. At this point, the strain is mainly concentrated in the step deformation zone with high shrinkage rate on the left side.

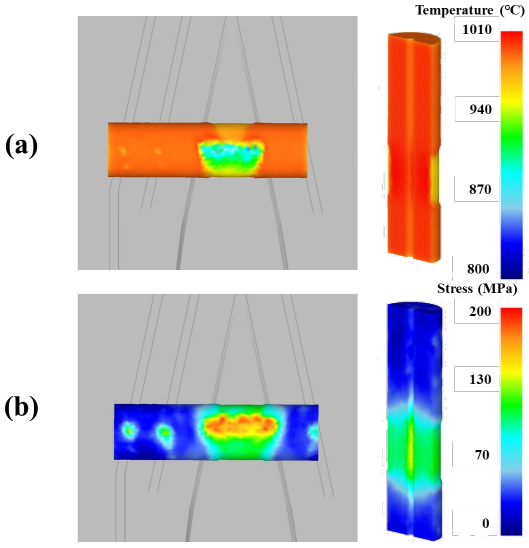

Fig. 5. Distribution of (a) temperature and (b) stress during CWR process (The beginning stage).

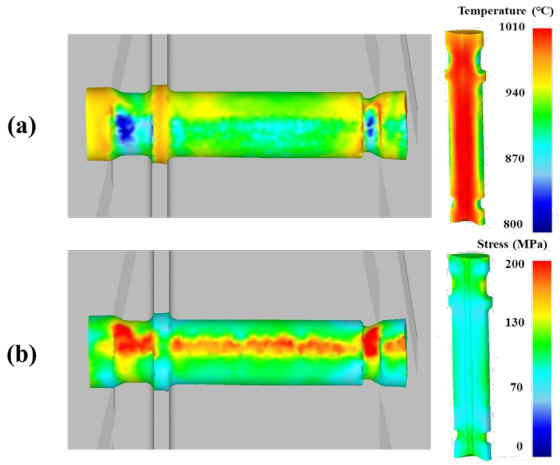

Fig. 6. Distribution of (a) temperature and (b) stress during CWR process (The intermediate stage).

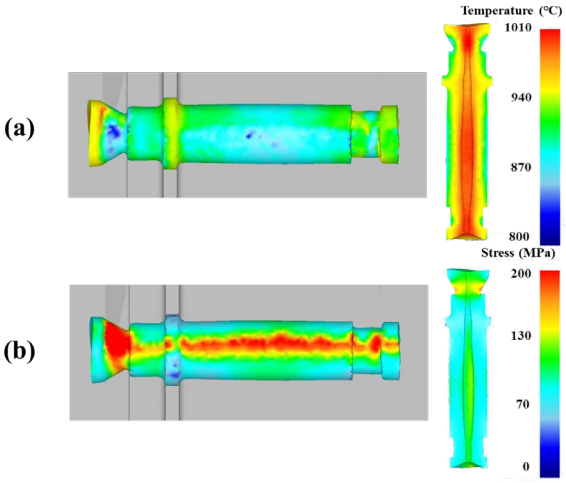

Fig. 7. Distribution of (a) temperature and (b) stress during CWR process (The end stage).

Fig. 8 shows the temperature and stress distribution on the cross-section of the rolled piece at different rolling stages. As the rolling progresses, the temperature gradually decreases from the core to the surface. And the stress is mainly concentrated in the area in contact with the tool. The position with the lowest temperature corresponds to the position with the highest stress, which makes the surface prone to damage. In the final stage, the deformation and stress are relatively large, which leads to the inner hole being compressed into an elliptical shape.

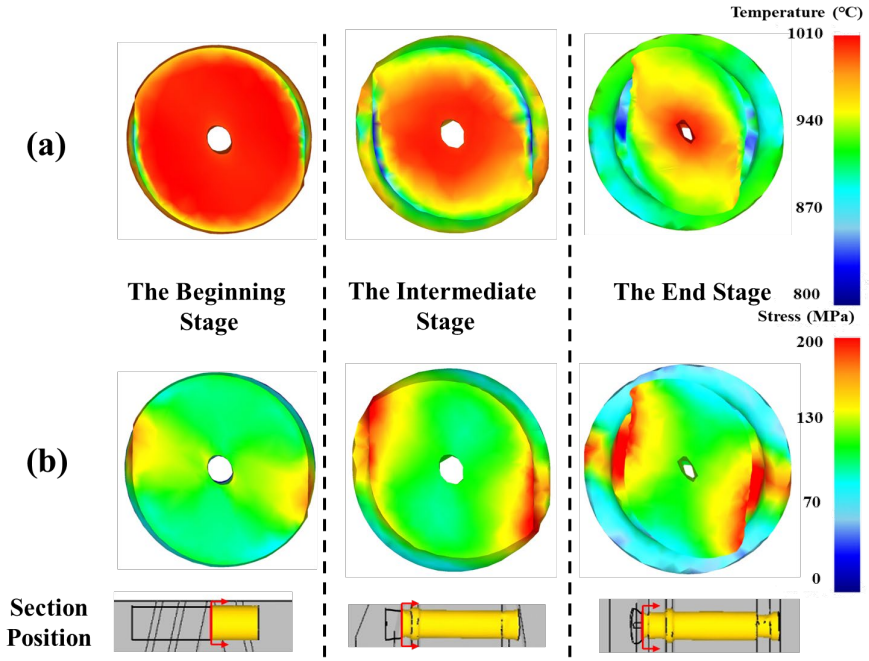

Fig. 8. Distribution of (a) temperature and (b) stress at cross section rolling piece during CWR process.

Analysis on the cross-section of the billet. Set six tracking points P1-P6 on the cross-section of the billet (Fig. 9), and then extract the temperature, stress, and strain of each point for comparative analysis to observe the trend of the forming process. The position selected for the cross-section is the position of wedging at the beginning of rolling, and the selection of this section is because it is the initial material segmentation position.

The temperature variation curves of each tracking point over time are shown in Fig. 10(a). It is observed that the temperature decreases more significantly as the distance from the center of the rolled piece increases, and the fluctuation of surface temperature becomes more pronounced as it approaches the center. This is due to the cyclic contact between the rolled piece and the colder tool. Due to the conversion of deformation work into thermal energy, the center temperature of the rolled piece shows a trend of first increasing and then decreasing, with a maximum temperature of 1040℃. The temperature curve at points P1-P4 shows a similar trend, indicating that the changes occurring during the deformation process are similar. Higher temperatures may lead to coarsening of the grain structure in the center of the rolled piece; And point P6 exhibits a very obvious temperature drop feature, and its temperature state exhibits significant fluctuations due to the rotation of the rolled piece.

Fig. 10(b) shows the variation curve of effective strain over time for each tracking point. Analyzing the curve, it can be observed that although the distance between the six tracking points is uniformly distributed, the strain is not uniform. The closer to the surface, the greater the increase in strain. This is because most of the deformation is carried out on the outer layer of the rolled piece. The strain at all six points shows a stage of drastic increase, and then the rolling proceeds to the finishing section. The curves of P1 and P2 are basically similar, belonging to the area with small deformation in the center, P2, P3, and P4 belong to the intermediate transition area, and P6 belongs to the area with the highest surface deformation. Compared with Fig. 11(a), it is found that the area of temperature cycling is also the area with the highest deformation, which may lead to defects such as cracks on the surface of the rolled piece.

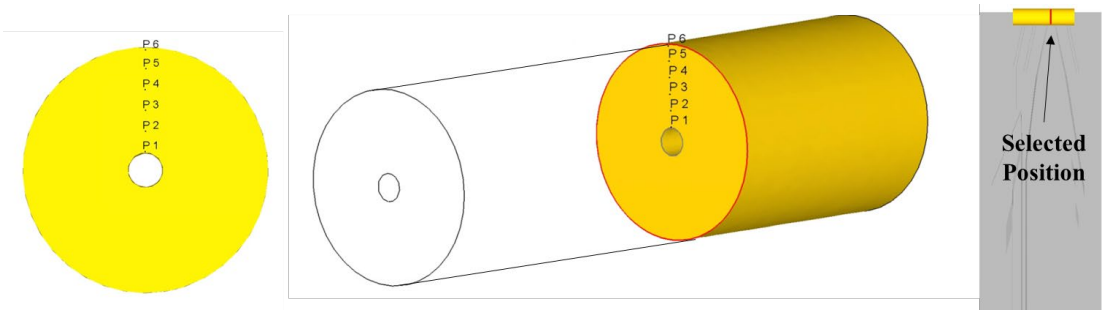

Fig. 9. Position of tracking points before rolling.

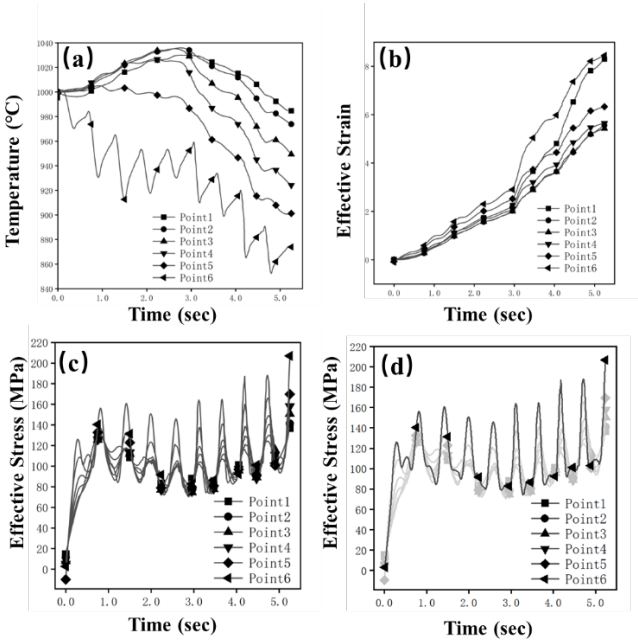

Fig. 10. The curves of temperature, effective strain and effective stress of tracking points over time.

Fig. 10(c) and (d) show the variation curves of effective stress at each tracking point over time. Analyzing the curve, it can be found that the stress at each point during the rolling process is roughly distributed in a wave shape, and the closer it is to the surface, the greater the amplitude of the wave. The fluctuation of stress is exactly opposite to the fluctuation of temperature. When the temperature is low, the stress is high, which may lead to damage.

Damage analysis. In the spreading section of the tool, the surface temperature of the rolled piece decreases and significant plastic deformation occurs, which may lead to cracking of the billet. The damage situation during the rolling process of the rolled piece is shown in Fig. 11. When the rolled piece contacts the wedge tip, damage begins to occur, and the damage value rapidly increases as the rolled piece enters the spreading section. To avoid the occurrence of cracks, it is necessary to optimize the widening section of the tool. While the widening angle should not be too large, the influence of the forming angle should also be considered.

For the center of the rolled piece, the damage increases with the elongation of the rolled piece, and the maximum damage value is located at the initial wedging position. This also corresponds to the position with the largest inner hole size.

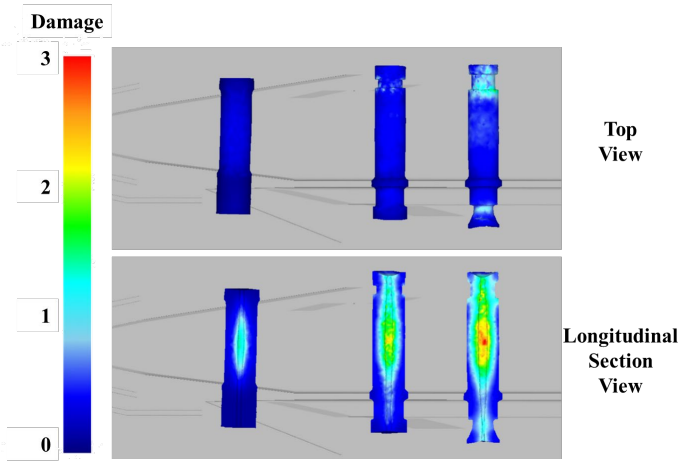

Fig. 11. Damage distribution during CWR process.

Summary

In this paper, the CWR preforming process of hollow motor shaft was studied, The main conclusions are as follows:

1. Hollow motor shaft can be produced through flat CWR technology at a rolling speed of 300 mm/s and a rolling temperature of 1000 ℃.
2. The surface dimension deviation not exceeding 0.8%, the maximum and minimum size of the inner hole are 14.6 mm and 3.4 mm, respectively;
3. Steps with high cross-sectional shrinkage are prone to damage, and the corresponding inner holes are prone to elliptical shapes;
4. The damage in the inner hole area is mainly concentrated at the initial wedged position, which is related to the elongation of the rolled piece.

Acknowledgment

This work was financially supported by the International Science and Technology Cooperation Project in Liaoning Province of China (Grant No. 2022JH2/10700006, 2023JH2/10700014), the National Key R&D Plan of China (Grant No. SQ2018YFE0119600) and the Sino-Belarus Inter-Governmental S&T Cooperation project (Grant No. CB02-09).

References

[1] Z. Pater, J. Tomczak, T. Bulzak, J. Bartnicki, A. Tofil, Prediction of Crack Formation for Cross Wedge Rolling of Harrow Tooth Preform, Materials 12 (2019) 2287-2287. https://doi.org/10.3390/ma12142287

[2] P.A. Li, B.Y. Wang, C. Yang, H. Zhang, W. Li, J. Zhou, Study on necking defects, microstructure and mechanical properties of TC4 alloy by cross wedge rolling, Int. J. Mater. Forming 15 (2022). https://doi.org/10.1007/s12289-022-01718-z

[3] Z.M. Yu, W.F. Peng, X. Zhang, M. Oleksandr, V. Titov, Evolution of microstructure of aluminum alloy hollow shaft in cross wedge rolling without mandrel, J. Central South University 29 (2022) 807-820. https://doi.org/10.1007/s11771-022-4950-8

[4] X. Ren, Y.M. Huo, S.R.E. Hosseini, T. He, Z. Yan, F.A.O. Fernandes, A.B. Pereira, H. Ji, J. Bai, Z. Bian, X. Du, A multi-scale modelling by coupling cellular automata with finite element method and its application on cross-wedge rolling, Materials Today Commun. 37 (2023) 106976. https://doi.org/10.1016/j.mtcomm.2023.106976

[5] T. Bulzak, Assessment of the Susceptibility to Material Fracture in the Cross-Wedge Rolling Process with Concave Tools, Materials 15 (2022) 6605-6605. https://doi.org/10.3390/ma15196605

[6] A.Q. Tian, X.H. Xu, L. Sun, Y.L. Deng, Effects of interrupted ageing and asymmetric rolling on microstructures, mechanical properties, and intergranular corrosion behavior of Al-Mg-Si-Zn alloy, J. Central South University 29 (2002) 821-835.

[7] Z. Pater, T. Bulzak, J. Tomczak, Cross-Wedge Rolling of Driving Shaft from Titanium Alloy Ti6Al4V, Key Eng. Mater. 3939 (2016) 687-687. https://doi.org/10.4028/www.scientific.net/KEM.687.125

[8] Z. Pater, J. Tomczak, Experimental Tests for Cross Wedge Rolling of Forgings Made from Non-Ferrous Metal Alloys, Arch. Metall. Mater. 57 (2012) 919-928. https://doi.org/10.2478/v10172-012-0101-9

[9] Z. Pater, J. Tomczak, T. Bulzak, Rotary compression as a new calibration test for prediction of a critical damage value, J. Mater. Res. Tech. 9 (2020) 5487-5498. https://doi.org/10.1016/j.jmrt.2020.03.074

[10] P.A. Li, B.Y. Wang, P.N. Feng, J. Shen, J. Wang, Numerical and experimental study on the hot cross wedge rolling of Ti-6Al-4V vehicle lower arm preform, Int. J. Adv. Manuf. Tech. 118 (2021) 3283-3301. https://doi.org/10.1007/s00170-021-07979-3

[11] L.F. Lin, W.F. Peng, S. Zhu, Z. Wu, J. Zhu, Y. Shao, H. Li, M. Oleksandr, V. Titov, Cross wedge roll bonding process for laminated shafts forming: Interface microstructure, bonding mechanism, and parameter influence, J. Mater. Process. Tech. 317 (2023). https://doi.org/10.1016/j.jmatprotec.2023.117971